Ferromagnetism and high Curie temperature in semiconductor heterostructures with Mn δ-doped GaAs and p-type selective doping

Ahsan M. Nazmul,* S. Sugahara, and M. Tanaka[†]

Department of Electronic Engineering, The University of Tokyo, 7-3-1 Hongo, Bunkyo-ku, Tokyo 113-8656, Japan
and PRESTO, Japan Science & Technology Corporation, 4-1-8 Honcho, Kawaguchi, Saitama 332-0012, Japan

The interaction between the magnetic dopants (Mn) and 2-dimensional hole gas (2DHG) in Mn δ-doped GaAs/Be-doped p-type AlGaAs heterostructures, where holes were supplied from the Be-doped AlGaAs to the Mn δ-doped GaAs, realized ferromagnetic ordering. The Curie temperature T_C of the heterostructure prepared with suitable growth conditions was 172 K, highest among the T_C values reported in III-V (InAs, GaAs) magnetic semiconductors.

Advances in epitaxial growth technology, such as molecular beam epitaxy (MBE), have made it possible to grow a variety of semiconductor heterostructures with atomically controlled layer thicknesses and abrupt doping profiles, in which the wave function of carriers can be controlled in artificially designed potentials.[1] This has led to creation of some electronic and optical devices, e.g. high-electron-mobility transistors (HEMT) and quantum-well lasers. While the bandgap and wave function engineering are so far limited to *nonmagnetic* semiconductor heterostructures, we aim to broaden its use to *magnetic* heterostructures and to extend the degree of freedom in designing spin-related properties in semiconductors. In this Rapid Communication, we use the two-dimensional hole gas (2DHG) system in selectively-doped GaAs/p-AlGaAs heterostructures[2] together with δ-doping of magnetic (Mn) impurities, and successfully maximize the ferromagnetic order among the Mn spins in GaAs by overlapping the wave function of 2DHG with the Mn δ-doping profile.

The mainstream studies of spin-electronic materials based on III-V semiconductors consist of (i) ferromagnet/semiconductor heterostructures such as MnAs/GaAs[3] and (ii) magnetic alloy semiconductors such as InMnAs and GaMnAs.[4–6] Despite extensive studies, in the former system special techniques are required to grow multilayer heterostructures with abrupt interfaces,[7] and much higher Curie temperature T_C is needed for practical application in the latter system [the highest T_C for the past few years was 110 K for (GaMn)As].[8] Unlike the random alloy system, here we use δ-doping of Mn in GaAs, where the doping profile along the growth direction is approximated by Dirac's δ-function. Inherent advantages of δ-doping[9] are locally high dopant concentration and high carrier concentration, which can lead to high Curie temperature T_C.[10] Another prospective advantage is easy fabrication of multilayer heterostructures containing Mn δ-doped GaAs layers with excellent interfaces.[11,12]

Mn δ-doped GaAs layers were grown on semi-insulating (SI) GaAs(001) substrates by MBE at the growth temperatures $T_s = 200–400\,°C$, and were characterized by secondary ion mass spectroscopy (SIMS), transmission electron microscopy (TEM), and X-ray standing wave studies. These structural analyses revealed that most of the Mn atoms are abruptly confined within a width of 2–3 monolayers (ML) in the zinc-blende structure as substitutional dopants, when the nominal thickness θ_{Mn} of Mn is below 1 ML.[12,13] The Mn doping profiles retained abruptness even at elevated T_s up to $400\,°C$. Here, $\theta_{Mn} = 1$ ML corresponds to a sheet Mn concentration of 6.3×10^{14} cm^{-2}, taking into account that Mn atoms are substituted for the Ga sublattice in the zinc-blende GaAs with the lattice constant of 0.565 nm. Although it was possible to incorporate high Mn concentration in the Mn δ-doped GaAs layers, the hole to Mn concentration ratio p/θ_{Mn} was very low and was not enough to realize ferromagnetic ordering.[13]

In order to obtain high hole concentration and locally high Mn concentration at the same position, we have grown 0.3 ML Mn δ-doped GaAs/Be-doped p-AlGaAs heterostructures by MBE, its structure is shown in Fig. 1(a). These p-type selectively doped heterostructures (p-SDHS) resemble an inverted high electron mobility transistor, where holes are provided from the p-AlGaAs layer to the overlying GaAs layer. A 200 nm-thick undoped GaAs buffer layer, a 300 nm-thick undoped Al$_{0.3}$Ga$_{0.7}$As layer, a 30 nm-thick Be-doped p-Al$_{0.3}$Ga$_{0.7}$As (Be concentration was 1.8×10^{18} cm^{-3}), and a d_s nm-thick undoped GaAs separation layer were successively grown at $T_s = 600\,°C$ on a SI-GaAs(001) substrate. Then, 0.3 ML Mn was deposited with a 20 nm-thick undoped GaAs cap layer at $T_s = 400\,°C$ or $300\,°C$. The thickness d_s of the undoped-GaAs separation layer was a measure to control the interaction between the Mn δ-doped GaAs layer and the 2DHG formed at the GaAs/p-AlGaAs interface. Successful epitaxial growth of the p-SDHS was confirmed by *in situ* reflection high-energy electron diffraction (RHEED) observations. A cross sectional high-resolution TEM lattice image of a 1 ML Mn δ-doped GaAs layer in Fig. 1(b) (grown at $T_s = 300\,°C$) shows that Mn atoms are incorporated in the zinc-blende structure without any dislocations or clusters. Other TEM images suggest that the δ-doped Mn atoms are localized within a width of 2–3 ML.[12]

Hall loops (Hall resistance versus magnetic field B) at 40 K of 0.3 ML Mn δ-doped GaAs layers grown at $400\,°C$ *without* and *with* p-SDHS ($d_s = 3$ nm) are shown in Figs. 2(a) and 2(b), respectively. The hysteresis in the Hall loop of the sample *with* p-SDHS clearly indicates ferromagnetic order, while the ferromagnetic hysteresis is absent in the sample *without* p-SDHS. The origin of the negative slope at
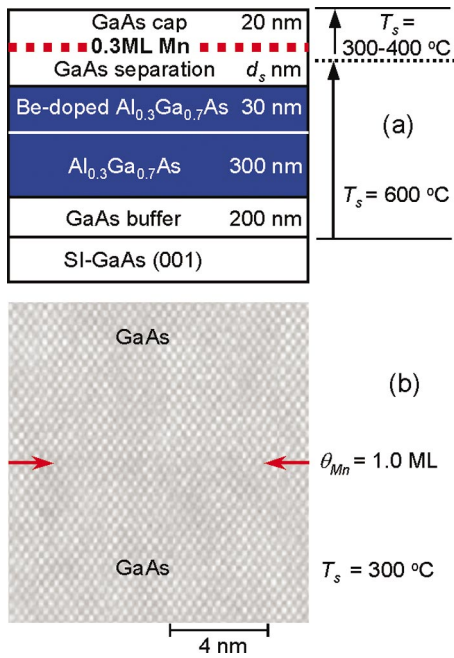
FIG. 1. (Color) (a) Sample structure of Mn δ-doped GaAs *with* *p*-type selectively doped heterostructures (*p*-SDHS). The GaAs separation layer thickness d_s was 0–10 nm. Holes are supplied from the Be-doped *p*-type $Al_{0.3}Ga_{0.7}As$ layer to the Mn δ-doped GaAs layer in the SDHS. (b) High-resolution TEM lattice image of the Mn δ-doped GaAs layer with $\theta_{Mn}=1.0$ ML grown at $T_s=300\,°C$.

FIG. 2. (Color) (a), (b) Hall loops of 0.3 ML Mn δ-doped GaAs layers grown at $400\,°C$ *without* and *with* *p*-SDHS ($d_s=3$ nm), measured at 40 K. (c) $R_{sheet}-T$ traces of the samples *without* and *with* *p*-SDHS, respectively. (d) $R_{sheet}-T$ traces of 0.3 ML Mn δ-doped GaAs samples *with* *p*-SDHS for $d_s=0$, 3, 5 and 10 nm. (e) Schematic diagram of the valence band profile of the *p*-SDHS, the 2DHG wave function, and Mn dopants. E_V and E_F are the valence band top and the Fermi energy, respectively. z is the growth direction.

$B>2$ kG in Fig. 2(b) is the influence of the negative magnetoresistance, which is proportional to the Hall resistivity. Details of the expressions are described later. The temperature dependence of the sheet resistance ($R_{sheet}-T$) of the samples *without* and *with p*-SDHS is plotted in Fig. 2(c). The sample *without p*-SDHS shows insulating behavior due to the low hole concentration as described earlier. In contrast, the sample *with p*-SDHS shows a local maximum of the $R_{sheet}-T$ trace, which suggests that T_C is around 70 K. This value of T_C was confirmed by measuring Hall loops at various temperatures, where hysteresis remained open up to 60–70 K.

The ferromagnetic order of the samples *with p*-SDHS was found strongly dependent on the GaAs separation layer thickness d_s. As shown in Fig. 2(d), the local maximum temperature of the bump in the $R_{sheet}-T$ trace, which roughly corresponds to T_C, was 45 K at $d_s=0$ nm and 70 K at $d_s=3$ nm. The Hall loops showed clear ferromagnetic hysteresis at $d_s=0$ and 3 nm below T_C. With further increase of d_s to 5 and 10 nm, the bump disappeared. Hysteresis in loops was not observed at $d_s=5$ and 10 nm, indicating the absence of ferromagnetic order. The d_s dependence of the ferromagnetic order is explained using the valence band diagram of the heterostructure in Fig. 2(e). Here, z is the growth direction of the sample. The concentration of 2DHG formed at the GaAs/*p*-AlGaAs heterointerface without Mn δ-doping was 1.8×10^{12} cm^{-2}, estimated by Hall measurements. We think that the degree of the overlap of the 2DHG wave function and the Mn δ-doping profile directly affects the ferromagnetic ordering and T_C of the heterostructures. T_C was highest
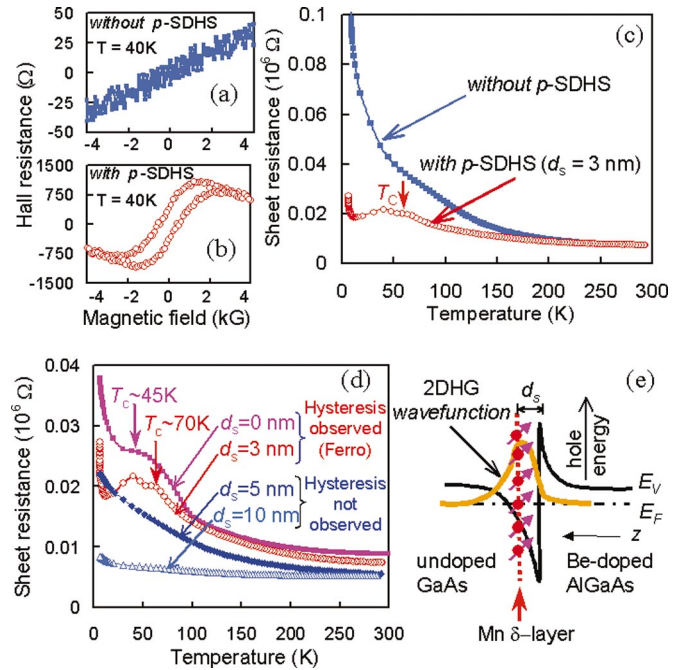
(70 K) at $d_s=3$ nm, because the overlap was maximum. Note that the self-consistent calculation of GaAs/*p*-AlGaAs heterostructures[14] indicates that the peak position of the 2DHG wave function with similar order of hole concentration to ours is around 3 nm away from the heterointerface, which is in good agreement with our explanation. Further increase of d_s to 5 and 10 nm decreased the overlap of the 2DHG wave function and the Mn δ-doping profile, thus weakened the ferromagnetic order. We also notice that the sheet resistance R_{sheet} of the Mn δ-doped GaAs heterostructures decreased with the increase of d_s [see Fig. 2(d)]. It is apparent that d_s plays the role of controlling the degree of scattering of the 2DHG by the Mn dopants in the δ-doped layer. The increase of d_s weakens the scattering, thus increases the mobility of the 2DHG and eventually decreases R_{sheet}.

In order to completely suppress the surface segregation of Mn, and to obtain locally higher Mn concentration in a ideally sharp δ-doped profile, T_s of the Mn δ-doped GaAs layer in the SDHS was lowered from $400\,°C$ (at which surface segregation of around 30% Mn dopants was observed in the SIMS depth profile) to $300\,°C$ (at which no segregation of Mn was detected).[12,13] The sample examined here was a 0.3 ML Mn δ-doped GaAs ($T_s=300\,°C$)/Be-doped *p*-AlGaAs heterostructure with $d_s=0$ nm, as shown in Fig. 1(a).

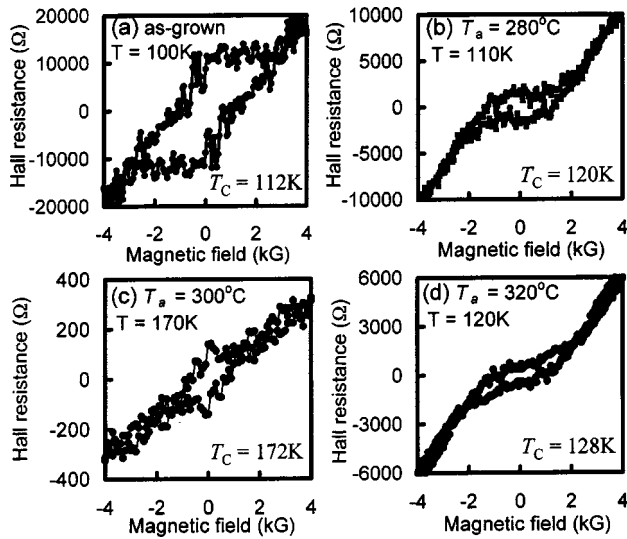It is known that the transport and magnetic properties of III-V magnetic semiconductors are very sensitive to the

FIG. 3. Ferromagnetic Hall hyteresis loops of a 0.3 ML Mn δ-doped GaAs layer *with p*-SDHS ($d_s=0$ nm) grown at 300 °C; (a) as-grown sample measured at 100 K, (b) sample with T_a = 280 °C measured at 110 K, (c) sample with T_a = 300 °C measured at 170 K, and (d) sample with T_a = 320 °C measured at 120 K.

growth conditions,[15] and also to low temperature (LT) annealing (at temperatures slightly above the growth temperature).[16] We expect a similar effect for the Mn δ-doped GaAs layer grown at $T_s=300$ °C *with p*-SDHS. LT-annealing was carried out in a nitrogen atmosphere for 15 minutes with various annealing temperatures $T_a=280$, 300, 320, and 335 °C. Figure 3 shows the Hall loops of the as-grown and annealed samples. The hysteresis in the Hall loop in Fig. 3(a) indicates ferromagnetism at 100 K in the as-grown sample. Remarkable improvement of T_C was achieved in the annealed samples [Figs. 3(b)–(d)]. Especially, the hysteresis in Fig. 3(c) indicates that the ferromagnetic order is retained even at 170 K for the sample annealed at T_a = 300 °C. Further increase of T_a to 320 °C resulted in the fall of T_C [Fig. 3(d)]. Note that T_C was increased from 70 K (grown at $T_s=400$ °C, as-grown) to 112 K ($T_s=300$ °C, as-grown), and 172 K ($T_s=300$ °C, LT-annealed). Our explanation is that while the partially segregated Mn dopants at T_s = 400 °C do not take part in the ferromagnetic ordering, the more abrupt profile of Mn dopants with higher peak concentration grown at 300 °C resulted in the increase of T_C. This T_C was further enhanced by the LT-annealing, which contributed to the reduction of point defects and thus led to lower compensation.

In order to estimate T_C and the hole concentration p of the sample by ruling out the anomalous Hall effect, we have performed the Curie Weiss fitting to the experimental trace of Hall resistivity ρ_H (or Hall coefficient R_H) versus temperature T. In a magnetic material, there exists the anomalous Hall effect contribution to the Hall resistivity, expressed as $\rho_H = R_O B + R_S M$, where R_O is the ordinary Hall coefficient, B is the magnetic field, R_S is the anomalous Hall coefficient and M is the magnetization of the sample.[17] R_S is proportional to the resistivity ρ of the sample, $R_S = c\rho$ (c is a constant), when skew-scattering is dominant. On the other hand,
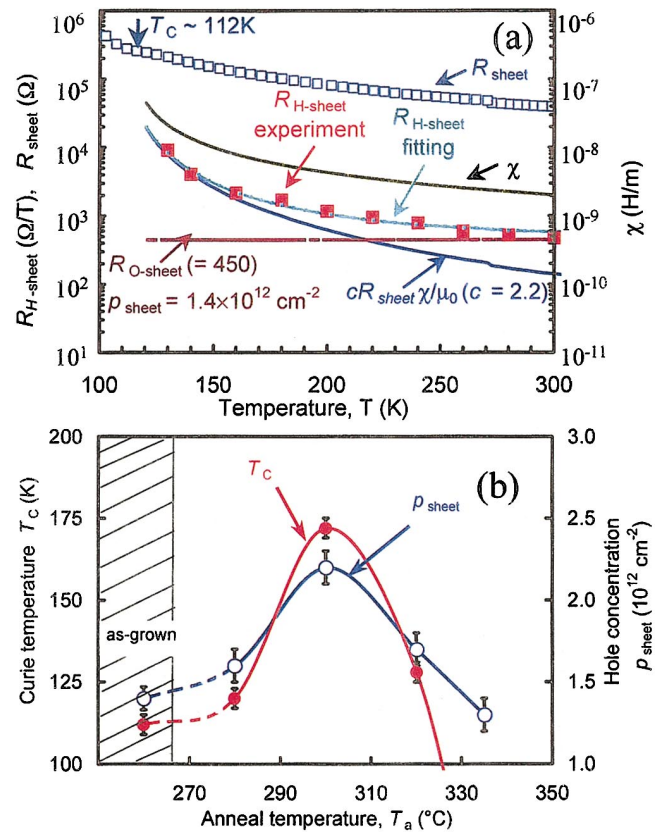

FIG. 4. (Color) (a) Temperature dependence of the sheet resistance R_{sheet} (open squares) and sheet Hall coefficient $R_{H\text{-}sheet}$ (filled squares) of the as-grown 0.3 ML Mn δ-doped GaAs ($T_s=300$ °C) *with p*-SDHS. From the Curie Weiss fitting to the $R_{H\text{-}sheet}-T$ curve, $R_{O\text{-}sheet}$ and χ are estimated, yielding $p_{sheet}=1.4\times10^{12}$ cm^{-2} and $T_C=112$ K. Here, $R_{H\text{-}sheet}=R_{O\text{-}sheet}+cR_{sheet}\chi/\mu_0$, where $R_S = cR_{sheet}$ and $\chi=C/(T-T_C)$. (b) T_C (filled circles) and p_{sheet} (open circles) as a function of T_a. The as-grown results are connected with dotted lines.

the magnetization in the paramagnetic state ($T \gtrsim T_C$) is expressed as $M=\chi H=\chi B/\mu_0$, where the magnetic susceptibility χ follows the Curie Weiss law, $\chi=C/(T-T_C)$, and C is the Curie constant. By taking into account the general Curie Weiss equation, the Hall coefficient R_H is expressed as $R_H = \rho_H/B = R_O + c\rho\,C/\mu_0(T-T_C)$. The fitting using this equation to the experimental R_H-T trace yields the T_C and p ($=1/eR_O$; e is the charge of a hole).

It is notable that the Curie constant C of magnetic semiconductors is theoretically expressed as $C=(4/a_0^3)\times(p_{eff}^2\mu_B^2 x)/(3k_B)$,[18] where μ_B is the Bohr magneton, k_B is the Boltzman constant, a_0 is the lattice constant (in our case, a_0 is set at 5.65 Å, which is the value for GaAs), x is the Mn content (x is set at 0.15 for $\theta_{Mn}=0.3$ ML, since we defined the local Mn content x as $\theta_{Mn}/2$ ML, where 2 ML is the width of the Mn distribution estimated by TEM), p_{eff} is the effective magnetic moment of a Mn ion (defined as $p_{eff}=g[S_{Mn}(S_{Mn}+1)]^{1/2}$; g and S_{Mn} are the g-factor and the total spin of Mn). In our analysis, we used $g=2$, and $S_{Mn}=5/2$, which are the values of the (GaMn)As random alloy.[19] The above general equation of a bulk magnetic material can be modified to $R_{H\text{-}sheet}=R_{O\text{-}sheet}+cR_{sheet}C/\mu_0(T-T_C)$ for a

2-dimensional system, where $R_{\text{H-sheet}}$ is the sheet Hall coefficient, $R_{\text{O-sheet}}$ is the ordinary sheet Hall coefficient and R_{sheet} is the sheet resistance of the sample. From the fitting using the modified equation to $R_{\text{H-sheet}}$ measured at $T \geq T_C$, one can estimate $R_{\text{O-sheet}}$ ($R_{\text{O-sheet}} = 1/ep_{\text{sheet}}$), thus the sheet hole concentration p_{sheet}, and T_C.

Figure 4(a) shows the temperature dependence of R_{sheet} and $R_{\text{H-sheet}}$ of the as-grown 0.3 ML Mn δ-doped GaAs ($T_s = 300\,^\circ\text{C}$)/$p$-AlGaAs heterostructure. In the paramagnetic state of the sample ($T \geq T_C$), the experimental value of $R_{\text{H-sheet}}$ (in the Ohm/Tesla unit) is expressed as the slope of the linear relation of Hall resistance versus magnetic field B. Figure 4(a) also plots the Curie Weiss fitting to the experimental $R_{\text{H-sheet}} - T$ data measured at different temperatures ($T \geq T_C$), and also shows temperature dependent curves of χ $[=C/(T-T_C)]$, $R_{\text{O-sheet}}$, and $cR_{\text{sheet}}\chi/\mu_0$, needed for the Curie Weiss fitting. From the Curie Weiss fitting, it was estimated that T_C was 112 K, and p_{sheet} was 1.4×10^{12} cm^{-2}. The prefactor constant c was taken to be 2.2 T^{-1}. The estimated T_C of 112 K is in good agreement with the temperature dependence of the remanence of the Hall hysteresis loops at $T \leq T_C$. The T_C of samples annealed at $T_a = 280$, 300, and 320 °C, estimated in the same way, were 120, 172, and 128 K, respectively, which were also in good agreement with the temperature dependence of the remanence of the Hall hysteresis loops measured at $T \leq T_C$ (see Fig. 3). It is notable that the prefactor c existed between 1.8–2.2 T^{-1} for all the as-grown and annealed samples of Mn δ-doped GaAs heterostructures, which is comparable to the reported values of (In,Mn)As[20] ($c = 5.6$) and (Ga,Mn)As[5] ($c = 1.8$). Hence, the above-mentioned c values in the Mn δ-doped GaAs heterostructures can eliminate the possibility of superparamagnetism. Furthermore, the absence of any clusters in the high resolution lattice images of cross-sectional TEM [see Fig. 1(b)] also negates the possibility of superparamagnetism from tiny cluster structures.

In order to explain the remarkable enhancement of T_C due to the LT-annealing, T_C and p_{sheet} estimated by the Curie Weiss fittings are plotted as a function of annealing temperature T_a in Fig. 4(b). It is apparent that, up to $T_a = 300$ °C, the decrease of electrical compensation of holes by Mn interstitials or other defects resulted in the increase of the hole concentration and magnetically active Mn dopants, and thus enhanced 2DHG-mediated ferromagnetic ordering among the local Mn spins and increased its T_C. However, above 300 °C, diffusion of the Mn dopants might have resulted in the decrease of ferromagnetic ordering.

In summary, we have shown that the controlled overlap of the wave function of the 2DHG and the Mn δ-doping profile in GaAs can lead to ferromagnetic ordering. The highest T_C of the ferromagnetic heterostructures prepared with suitable growth conditions and low-temperature annealing was 172 K. This T_C value is the highest among the reported values in III-V (GaAs, InAs) magnetic semiconductors.

---

*Electronic address: ahsan@cryst.t.u-tokyo.ac.jp

†Electronic address: masaaki@ee.t.u-tokyo.ac.jp

[1] H. Sakaki, *Molecular Beam Epitaxy*, in *III-V Semiconductor Materials and Devices*, edited by R.J. Malik (Elsevier Science, Amsterdam, 1989), pp. 217–330.

[2] H. L. Stormer and W. T. Sang, Appl. Phys. Lett. **36**, 685 (1980); H. L. Stormer, A. C. Gossard, W. Wiegmann, R. Blondel, and K. Baldwin, Appl. Phys. Lett. **44**, 139 (1984).

[3] M. Tanaka, J. P. Harbison, T. Sands, T. L. Cheeks, and G. M. Rothberg, J. Vac. Sci. Technol. B **12**, 1091 (1994); M. Tanaka, J. P. Harbison, and G. M. Rothberg, Appl. Phys. Lett. **65**, 1964 (1994); M. Tanaka, Semicond. Sci. Technol. **17**, 327 (2002).

[4] H. Munekata, H. Ohno, S. von Molnar, Armin Segmuller, L. L. Chang, and L. Esaki, Phys. Rev. Lett. **63**, 1849 (1989).

[5] H. Ohno, A. Shen, F. Matsukura, A. Oiwa, A. Endo, S. Katsumoto, and Y. Iye, Appl. Phys. Lett. **69**, 363 (1996).

[6] M. Tanaka, J. Vac. Sci. Technol. B **16**, 2267 (1998).

[7] M. Tanaka, K. Saito, and T. Nishinaga, Appl. Phys. Lett. **74**, 64 (1999).

[8] F. Matsukura, H. Ohno, A. Shen, and Y. Sugawara, Phys. Rev. B **57**, R2037 (1998); More recently higher T_C (140 K) is reported in K. W. Edmonds, K. Y. Wang, R. P. Campion, A. C. Neumann, N. R. S. Rarley, B. L. Gallagher, and C. T. Foxon, Appl. Phys. Lett. **81**, 4991 (2002), and T_C (150 K) in K. C. Ku, S. J. Potashnik, R. F. Wang, S. H. Chun, P. Schiffer, N. Samarth, M. J. Seong, A. Mascarenhas, E. Johnston-Halperin, R. C. Mayers, A. C. Gossard, and D. D. Awschalom, Appl. Phys. Lett. **82**, 2302 (2003).

[9] E. F. Schubert, J. M. Kuo, R. F. Kopf, H. S. Luftman, L. C. Hopkins, and N. J. Sauer, J. Appl. Phys. **67**, 1969 (1990).

[10] T. Dietl, H. Ohno, F. Matsukura, J. Cibert, and D. Ferrand, Science **287**, 1019 (2000).

[11] R. K. Kawakami, E. Johnston-Halperin, L. F. Chen, M. Hanson, N. Guebels, J. S. Speck, A. C. Gossard, and D. D. Awschalom, Appl. Phys. Lett. **77**, 2379 (2000).

[12] Ahsan M. Nazmul, S. Sugahara, and M. Tanaka, J. Cryst. Growth **251**, 303 (2003); also, see EPAPS Document No. E-PRBMDO-67-R04324 for the auxiliary material. A direct link to this document may be found in the online article's HTML reference section. The document may also be reached via the EPAPS homepage (http://www.aip.org/pubservs/epaps.html) or from ftp.aip.org in the directory /epaps/. See the EPAPS homepage for more information.

[13] Ahsan M. Nazmul, S. Sugahara, and M. Tanaka, Appl. Phys. Lett. **80**, 3120 (2002).

[14] T. Ando, J. Phys. Soc. Jpn. **54**, 1528 (1985).

[15] H. Shimizu, T. Hayashi, T. Nishinaga, and M. Tanaka, Appl. Phys. Lett. **74**, 398 (1999).

[16] S. Katsumoto, T. Hayashi, Y. Hashimoto, Y. Iye, Y. Ishiwata, M. Watanabe, R. Eguchi, T. Takeuchi, Y. Harada, S. Shin, and K. Hirakawa, Mater. Sci. Eng., B **84**, 88 (2001).

[17] L. Berger and G. Bergmann, *The Hall Effect and Its Applications*, edited by C. L. Chien and C. R. Westgate (Plenum, New York, 1980), p. 55.

[18] J. K. Furdyna, J. Appl. Phys. **64**, R29 (1988).

[19] H. Ohno, J. Magn. Magn. Mater. **200**, 110 (1999).

[20] H. Ohno, H. Munekata, T. Penney, S. von Molnar, and L. L. Chang, Phys. Rev. Lett. **68**, 2664 (1992).